Stability Evaluation of Insulated Gate AlGaN/GaN Power Switching Devices Under Heavy-Ion Irradiation

Steve Stoffels, Michel Mélotte, Magali Haussy, Rafael Venegas, Denis Marcon, Marleen Van Hove, and Stefaan Decoutere

***Abstract*—Depletion mode insulated gate AlGaN/GaN power switching HEMTs were evaluated for stability under heavy-ion irradiation. Experiments were performed for different types of heavy-ion species, values of gate bias, drain bias, and device geometry. For the insulated gate AlGaN/GaN devices, an as-of-yet unobserved single-event occurred, which we have termed *single-event switching* (SES). These SES events occurred next to previously observed single-event gate rupture (SEGR) events. It was found that the SES events were gate leakage dependent and stopped occurring above a certain threshold value of gate leakage. Statistical analysis showed that the cross section for single SES events exhibited a lognormal distribution with a median value close to the gate area, and the capture cross section exhibited a slight voltage dependence. The gate leakage after irradiation, on the other hand, was exponentially distributed and was strongly voltage and geometry dependent, indicating an electric field dependency.**

***Index Terms*— AlGaN/GaN HEMT, Gallium nitride, heavy-ion irradiation, High-K gate dielectrics, MISHEMT, SEGR, SET.**

I. Introduction

HIGH-ELECTRON mobility transistors (HEMTs) fabricated from the AlGaN/GaN material system have promising applications in space due to the inherent strength of the material for different ionizing and nonionizing radiation types as indicated in previous work [1], [2]. In the literature, several tests have been performed on AlGaN/GaN high-electron mobility transistors, with either a Schottky gate architecture [3], [4] or an e-mode architecture with a p-type GaN material at the gate [5], [6]. The stability of HEMT transistors have been evaluated under proton irradiation, gamma irradiation, and heavy-ion irradiation. For all devices analyzed in the literature, no single-event burnout (SEB) events were detected [3], [4]. On the other hand, single-event gate rupture (SEGR) has been identified as the main degradation mechanism. It was shown that the degradation mechanism was voltage dependent, as shown in [3]. In that work, the devices were shown to be very robust to SEGR for low gate and drain biases, which explains why some authors did not observe SEGR [4] under heavy-ion irradiation.

In this work, we have tested, for the first time, the stability of a high voltage, metal–insulator–semiconductor high-electron mobility transistor (MISHEMT) under heavy-ion irradiation. The gate dielectric consisted of a novel, double dielectric stack [7] under the gate electrode. Gate leakage, threshold voltage, and on-resistance were monitored before and after irradiation with heavy ions. In other works, authors have used stepped-stress [8], single-point, or fluence-dependent measurements to evaluate the impact of irradiation on device performance. In this work, we have used statistical distribution functions on a population of samples to evaluate the impact of several experimental parameters on gate leakage. The advantage of this method is that it allows performing lifetime extractions of the components under irradiative degradation.

During the testing, the devices were biased in the off-state with a high drain voltage, as the high electrical fields under this condition have a strong negative impact on device reliability and the state is thus a critical state to investigate for power switching components. Using a gate dielectric has advantages for creating components with low gate leakage but can introduce extra problems when irradiated, such as charge trapping in the gate dielectric or dielectric rupture (SEGR) [9]. As a first step to evaluate the radiation hardness of the technology, we have performed high energetic heavy-ion irradiation with various ion species. The stability of the component for heavy-ion irradiation was evaluated by monitoring important device parameters, such as on-resistance $(\mathrm{R_{on}})$, threshold voltage $(\mathrm{V_t})$, gate, and drain leakage, before and after irradiation. The impact of gate and drain bias on the radiation damage was also evaluated as well as the effect of device geometry. It was found that the MISHEMTs suffered from an extra degradation mechanism, which is not commonly found in other AlGaN/GaN architectures which have been subjected to radiation testing. The new failure mechanism was a nondestructive single-event switching (SES) event, with a nonconstant capture cross section.

In the next section, we will first discuss the component, fabrication, and the experimental setup. The experiments and results will be detailed in the following section. An analysis and discussion of the results is performed in the next section. Finally, the paper will finish with the conclusions.

Manuscript received October 01, 2012; revised February 12, 2013, June 03, 2013, and July 01, 2013; accepted July 01, 2013. Date of publication August 06, 2013; date of current version August 14, 2013. This work was supported in part by the ESAproject GaN-In-Line, 20713/07/NL/SF .

S. Stoffels, R. Venegas, D. Marcon, M. Van Hove and S. Decoutere are with Imec, B-3001 Leuven, Belgium (e-mail: stoffels@imec.be).

M. Mélotte and M. Haussy are with Thales Alenia Space ETCA, B-6032 Charleroi, Belgium.

Color versions of one or more of the figures in this paper are available online at http://ieeexplore.ieee.org.

Digital Object Identifier 10.1109/TNS.2013.2272331

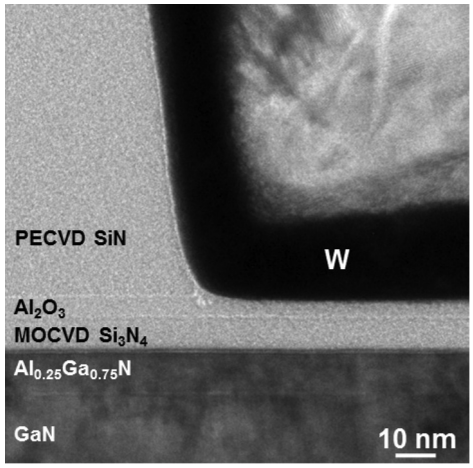

Fig. 1. TEM picture of the double dielectric gate stack for the MISHEMT.

II. Fabrication and Experimental Setup

For this paper, two different types of components were evaluated. The first type of components had a gate–drain distance $L_{gd} = 5\mu$m (type A) and the second a gate drain distance $L_{gd} = 16\mu$m (type B). Both components were two finger structures with a finger length of 500 μm (i.e., a total gate width of 1 mm).

The MISHEMT devices were fabricated in a silicon CMOS compatible fab on 6-in (111) silicon substrates. The epilayer stack was grown in a metal–organic chemical vapor deposition (MOCVD) tool and consisted of a 2.5-μm-thick AlGaN buffer, a 150-nm-thick GaN channel layer, a 10-nm $Al_{0.25}Ga_{0.75}N$ barrier layer and a 5 nm Si_3N_4 passivation layer. The *in-situ* grown Si_3N_4 layer is used to passivate the surface states and increase the channel electron concentration [10]. The gate was a double-layer dielectric stack consisting of a 5-nm *in-situ* Si_3N_4 combined with a 5-nm atomic layer deposition (ALD) deposited Al_2O_3 [7]. A transmission electron microscope (TEM) picture of the gate stack is shown in Fig. 1.

The components were packaged using wirebonding in the TAS ETCA ESA PSS10-606 qualified hybrid line. The goal of the radiation test was to evaluate the components in the off state, i.e., with low power dissipation. For this reason, a power package was not required. However, due to the small size of the components (1-mm total gate width), we expected a very fast reaction time and transients, which could lead to oscillations if parasitics are not kept under control. To reduce the risk of these problems, an SO-16 package was used, which allowed for traditional wire bonding and had short leads to reduce package parasitics. Two components were wirebonded per package; the packaged and bonded components are shown in Fig. 2.

The packaged components were then mounted in a test board, which included a 100-kΩ resistor on the drain side to prevent the device from destructive burnout, should an SEB occur (Fig. 3). The gate and drain biases were applied through the source monitor units (SMUs), SMU1 and SMU2, respectively. The SMUs were also used to periodically monitor I_g and I_d during the measurement, with a sampling time of 1.5 s. This allowed us to record I_g and I_d during the entire irradiation event, albeit with a rough time scale. An oscilloscope was also used to record

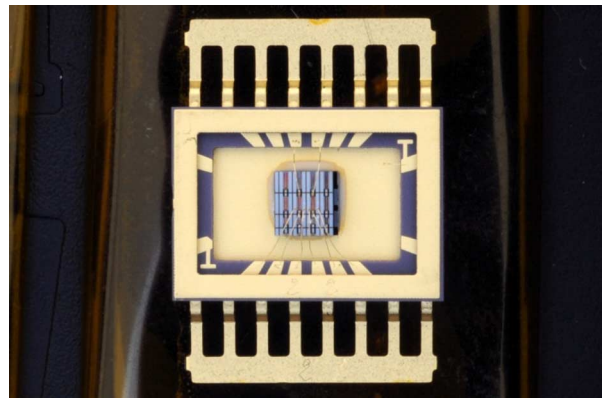

Fig. 2. Package of 2 GaN components (type A and type B) in an SO16 package.

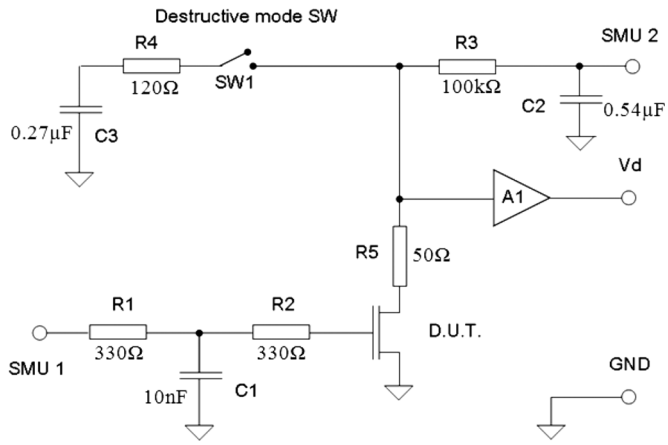

Fig. 3. Circuit used for testing the components. The component A1 is an attenuator with attenuation factor 250.

short time scale events at the drain level. The oscilloscope was connected to the terminal V_d. The attenuator A1 (attenuation factor of 250) in the circuit was used to attenuate the voltage to a safe level for the oscilloscope input. The oscilloscope was set to trigger on changes in V_d so that switching events on very short time scales could be recorded. Heavy-ion testing was performed following MIL-STD-750E, METHOD 1080. The components were irradiated at the cyclotron in Louvain-La-Neuve, Belgium. A picture of the setup is shown in Fig. 4. The sensitivity of the component to radiation damage was evaluated for different atomic species, namely Xe, Ar, Kr, and Ne. During the test run, the components were biased in the off state with a high voltage over the drain, ranging from 75 to 480 V. Both gate and drain bias were varied for different experiments to study the impact on the radiation damage. The gate leakage, threshold voltage and on-resistance were measured before and after the measurements with a parameter analyzer.

III. Experimental Results

Two different configurations of GaN power switching components were subjected to the radiation test. The first type of components had a gate–drain distance (L_{gd}) of 5 μm and the second an L_{gd} of 16 μm. The components were nominally identical for the rest. Safe operating voltages, derived from breakdown measurements, were first determined on devices

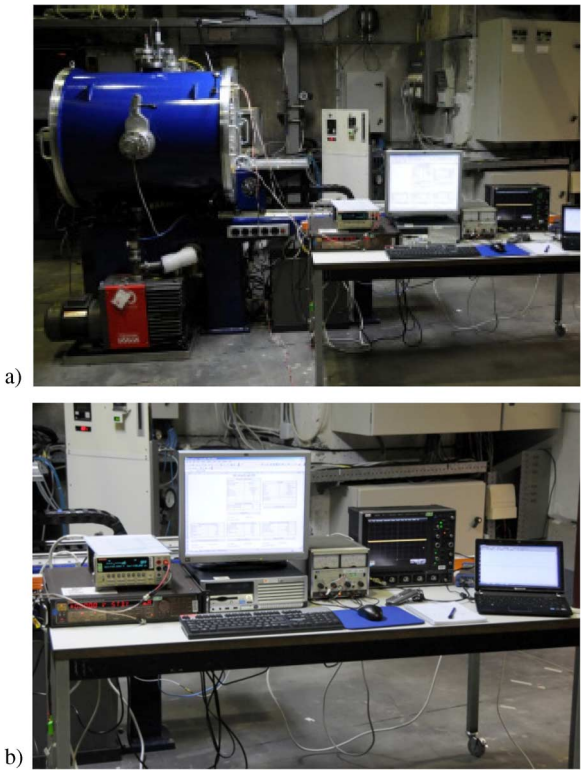

Fig. 4. Picture of the test setup: a) connected to the cyclotron NS b) close-up of the equipment.

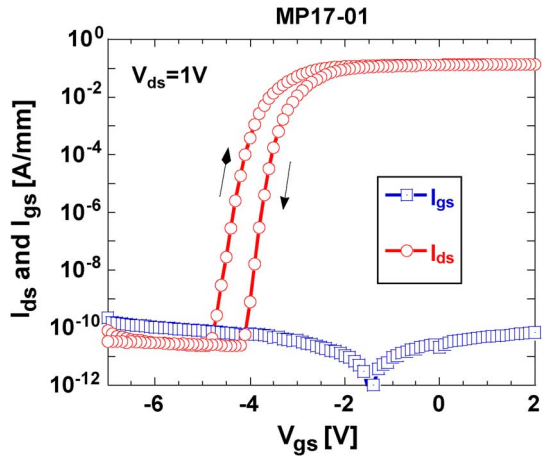

Fig. 5. Typical I_{ds}–V_{gs} characteristics measured before irradiation. An upward and downward sweep was performed to evaluate hysteresis.

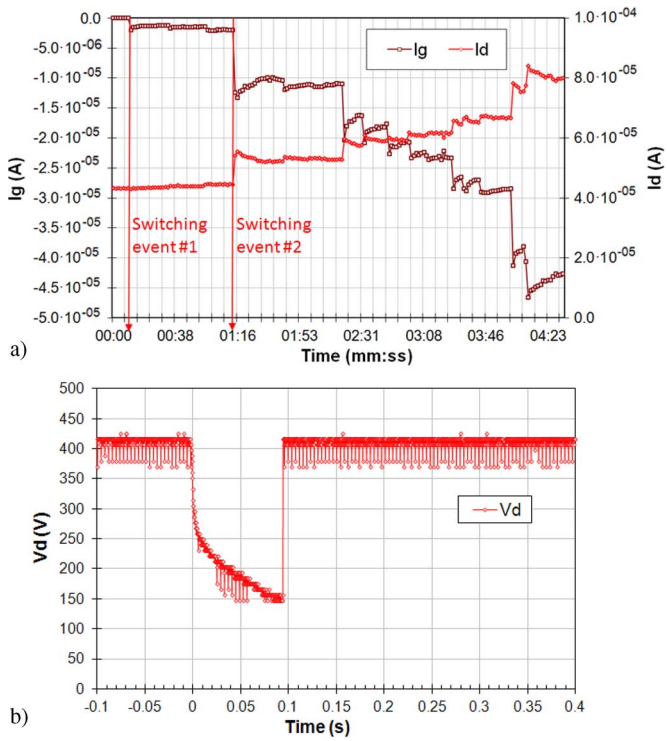

Fig. 6. a) Measurement of the Ig and Id during irradiation. This device had an L_{gd} of 16 μm. The device was irradiated with Kr (LET = 40.1 MeV/mg/cm^2), with a total fluence of 10^6 cm^{-2}. The device was biased at Vgs = −8 V and Vds = 410 V. b) Measurement of the voltage drop at the drain during the switching event 2, as measured with an oscilloscope after attenuating the voltage with a factor of 250.

with similar gate–drain distances. The safe operating voltage for the 5-μm device was 300 V, while the safe operating voltage for the 16 μm was 480 V. The I_{ds} and I_{gs} of the components were measured before subjecting them to the heavy-ion irradiation. The I_{ds} and I_{gs} characteristics were measured at V_{ds} = 1 V while sweeping the gate voltage from −6 to 2 V, both upward and downward sweeps were performed to evaluate hysteresis (Fig. 5). For these samples, the hysteresis was around 0.5 V. The V_T was around −4.5 V for both type of devices. It should be noted that GaN components are intrinsically depletion-mode devices, the high mobility channel is naturally present in the components due to polarization effects; therefore, the negative V_T is as expected.

We have subjected 48 samples to irradiation testing, half of the population of samples had a L_{gd} of 5 μm, while the other half had a L_{gd} of 16 μm.

The drain and gate currents were continuously monitored during radiation testing. It was observed that during irradiation, nondestructive single-event transients (SETs) occurred on the output voltage of the transistor [Fig. 6(b)], the voltage was measured at the terminal V_d in Fig. 3. It should be noted that measurements were performed with a protective resistor at the output, so destructive events could still occur without this resistor and should be evaluated in future experiments. The SET events manifested themselves as parasitic switching events, where the transistor started to conduct current without an external control of the gate potential and is different from the typical SEB in silicon, which occurs due to the switching on of a parasitic npn transistor in the component [9]. Due to the different mechanism we could speak of a SES event for the case of the GaN component.

During these SES events, there was a drop in the off-state voltage, as shown in Fig. 6(b). This indicates that there was a partial switching on of the transistor. From the voltage drop in Fig. 6(b) and the schematic circuit in Fig. 3, we can calculate the current going through the transistor and the channel resistance of the transistor during the event (the voltage drop is measured at the terminal Vd in Fig. 3). For the particular switching event, shown in Fig. 6(b), the current from drain to source was 2.6 mA,

giving a correlating resistance for the component of 58 kΩ. This indicates either a partial opening of the gate or a small localized switching event in a smaller region of the transistor. From the I_d–V_g relationship, it could be determined that a V_g around -4.7 V was needed to sufficiently open the gate to reach these values. The gate capacitance of this component was around 1pF in the off state; therefore, by using the relation $Q = C \cdot V$ ($Q =$ charge, $C =$ capacitance, $V =$ voltage), we could determine the charge on the gate during the SES event, which was around 3.3 pC.

The transient behavior of the component exhibited characteristics that are quite distinct from typical silicon powerMOS curves. For the GaN power transistor, we observed long switching, in the order of 0.1 s. Typical curves had on-state and off-state transient and a long plateau in between; however, no definitive correlation could be found. Both for the off-state and on-state transient, we could observe very steep transients for some cases, while in other cases, the rise or fall time of the voltage transient was much slower. Currently, it is not well understood why the curves exhibit this behavior; we expect that it is due to an accumulation of charge at the gate. Furthermore, for most cases, the switching events correlated with a permanent increase in the gate and drain–leakage current, which indicated that an SEGR occurred as shown in Fig. 6(a).

Unlike for Si power, these SESs did not occur continuously during irradiation, but rather the probability of the events to occur decreased after the first event. Thus, the capture cross section for the SES events was not constant and was correlated to the value of the gate leakage during irradiation (which increased due to the SEGR events). For higher gate leakage, the probability for SES events to occur decreased and above a certain threshold of gate leakage ($I_{g,tr}$), no further SES events could be observed. In practice, we observed an average of two to three switching events per experiment. We were able to determine the SES threshold for the gate leakage ($I_{g,tr}$), given by $I_{g,tr} = 30\ \mu$A. We have performed a statistical analysis to evaluate the capture cross section in our components. The capture cross section for a certain SES event can be calculated as

$$\frac{1}{\sigma} = \text{Fluence} \cdot \frac{\Delta t_{\text{SES}}}{t_{\text{run}}} \tag{1}$$

where σ [cm^2] is the capture cross section, Fluence [cm^{-2}] is the total fluence over the test run, t_{run} [s] is the duration of the test run and Δt_{SES} [s] is the time between two SES events (or the time to the first SES event from the start). It was found that the statistical distribution of the σ values for all events was lognormal (see Fig. 7). From this distribution, the sensitive area can be calculated, as it correlates to the median value of the lognormal distribution.

The sensitive area was calculated versus the gate leakage by binning the results for all measurements in three intervals of gate leakage. Namely, A: $I_g = 4 \cdot 10^{-12} - 8 \cdot 10^{-10}$ and B: $I_g = 8 \cdot 10^{-10} - 5.2 \cdot 10^{-6}$; C: $I_g = 5.2 \cdot 10^{-6} - 6.3 \cdot 10^{-4}$. For region A, the capture cross section was $1.4 \cdot 10^{-5}$, for region B, $\sigma = 1 \cdot 10^{-5}$cm^2, while for region C, the sensitive area decreased to $\sigma = 0.5 \cdot 10^{-5}$ cm^2, which indeed correlates with our observation that the amount of SES events decreased for higher values of gate leakage.

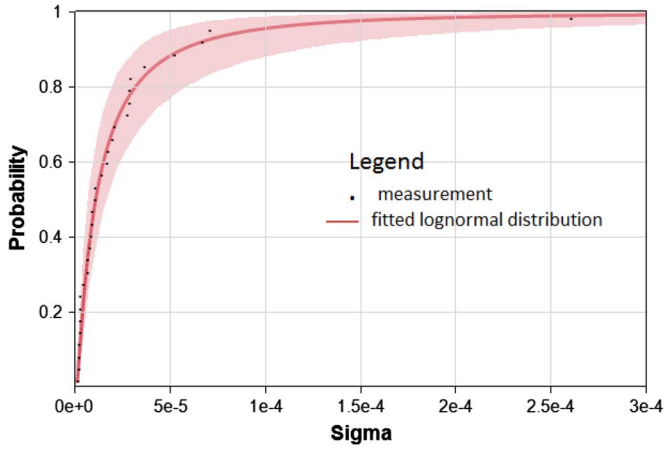

Fig. 7. Probability distribution for the calculated values of σ. A lognormal distribution has been fitted to the results, together with a 95% confidence interval.

The sensitive area was determined for Xe and Kr for $I_g < 1 \cdot 10^{-7}$, giving a $\sigma_{\text{Xe}} = 1.7 \cdot 10^{-5}$ cm^2 and $\sigma_{\text{Kr}} = 1.4 \cdot 10^{-5}$ cm^2. This capture cross section correlates to the area of the gate, which indicates that the SES events are most probably related to impacts at the gate area.

For Xe, the data was further refined versus V_{ds}. The sensitive area for $V_{ds} = 75$ V–240 V was $\sigma = 1.56 \cdot 10^{-5}$ cm^2, for $V_{ds} = 240$ V–410 V $\sigma = 2.11 \cdot 10^{-5}$ cm^2. These results seem to indicate that the sensitive area for SES events is voltage dependent. For GaN HEMT devices, the depletion region starts from the gate region and expands towards the drain terminal with increasing voltage. Therefore, the increased sensitive area could be related to the extension of the depletion region with voltage.

The total area of the exposed active area was $6.5 \cdot 10^{-5}$ cm^2 for the $L_{gd} = 5\ \mu$m design and $17.5 \cdot 10^{-5}$ cm^2 for the $L_{gd} = 16\ \mu$m design. The gate area was $1.5 \cdot 10^{-5}$ cm^2 for both type of devices. The value of the capture cross section is close to the value of the gate area and exhibits a slight voltage dependency, which seems to indicate that the events could be related to impacts in either the gate area or the depletion region in the component. However, more measurements would be needed to increase the confidence levels of the statistical analysis for the value for σ and its voltage dependency.

Above $I_{g,tr}$, no further SES events were observed; however, further degradation in I_g was still observed without the occurrence of switching events. In Fig. 6(a), this type of degradation can be observed for a time above two minutes, indicating that there are still SEGR type of events occurring during irradiation. The applied drain voltage V_{ds} and voltage over the component were continuously monitored during the experiment. With an increased leakage current of 30 μA, there was a maximum voltage drop of 3V over the protection resistor R3 (Fig. 3); therefore, the decrease in the number of switching events could not be related to a debiasing of the drain terminal of the transistor.

The degradation of the gate leakage under heavy-ion irradiation was studied in more detail. We have first verified the gate leakage ($I_{g,leak}$) before irradiation; this was done by performing several times a V_{ds} sweep from 0 V to the maximum safe operating voltage, while the device was biased in the off-state

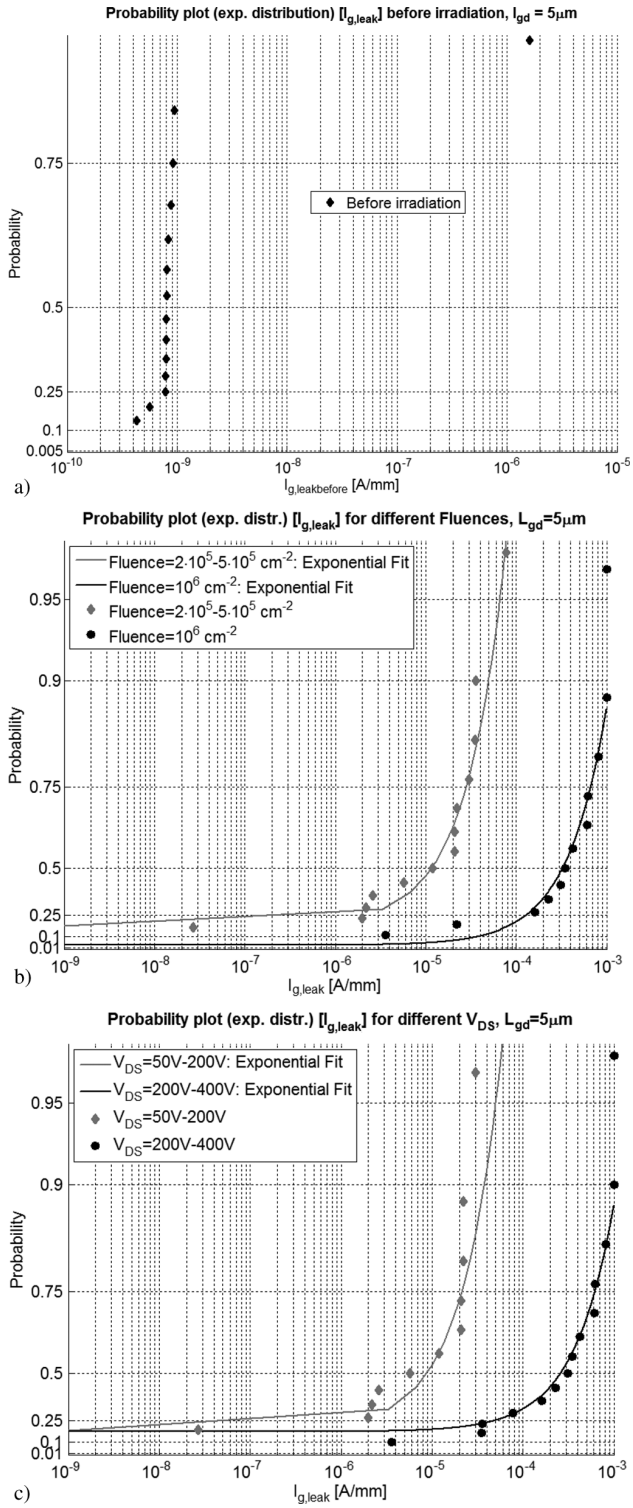

Fig. 8. Probability plot for an exponential distribution, calculated for the leakage current after irradiation ($(\mathrm{I_{g,leak}})$). Typical values for Ig,leak before irradiation were 10^{-10} A/mm. Probability plot for a) different fluences, b) for different drain biases for the devices with $\mathrm{L_{gd}} = 5\ \mu$m.

$(\mathrm{V_g} = -7\ \mathrm{V})$. Under these conditions, no degradation was observed of the leakage current, and there was a tight distribution of the $(\mathrm{I_{g,leak}})$ around 1 nA [Fig. 8(a)]. The degradation of the leakage under irradiation is a statistical process; therefore, we have used statistical distribution functions to compare the impact of several key parameters, plotting probability versus $\mathrm{I_{g,leak}}$. The probability in this graph is the percentage of components that has a lower leakage than the value of $\mathrm{I_{g,leak}}$ on the x-axis. We have found that the degradation of the gate current followed an exponential distribution law [11]. The effect of the fluence was studied first and, as can be seen in Fig. 8(b), we observed an increasing degradation for higher fluences. This indicates that a progressive degradation of the dielectric occurred for an increased number of particles hitting the component, as can be expected.

The device geometry and gate and drain bias were varied in a next step to study the impact of the electrical fields in the component. This is important, because when a high energetic ion traverses through the crystal, it leaves an electron–hole plasma in its wake. The biases applied to the component modify the energy structure in the semiconductor and thus the behavior of the generated electrons and holes. It was found that the gate bias did not have a discernable effect on the results, at least for the ranges in which it was varied for our experiments ($\mathrm{V_{gs}} = -8$ V to -3.6 V). However, for increasing drain bias, several effects could be observed. First of all, the data indicated a trend of increasing gate leakage after irradiation for a higher drain bias, shown in Fig. 8(b). Second, longer switching (SES) events could be observed (order of seconds), for a drain bias larger than 300 V. Devices exhibiting these long switching events were, however, still fully functional, as a postanalysis revealed. Third, in one instance, a destructive gate rupture was observed which rendered the component inoperable. This was observed for a 300-V rated device at 106% of its rated voltage. It was also found that the device with the smaller gate–drain distance of 5 μm exhibited more degradation, as can be seen in Fig. 9(a). For these devices, the high potential electrode is closer to the gate terminal, therefore increasing the electrical field. All these results indicate that the electrical fields in the component act as an acceleration factor for the radiation-induced gate degradation.

No definitive trend could be extracted for the increase of the on-resistance versus applied drain or gate bias during irradiation. Plotting the data versus ion species revealed, however, that the on-resistance exhibited a progressive degradation for the ions with higher atom number, as shown in Fig. 10. This degradation is indicative of either lattice damage in the GaN channel/buffer or degradation of the $\mathrm{Si_3N_4}$ passivation (either through lattice damage or charge trapping). The degradation of the gate leakage versus ion specify did not show a clear relationship versus atom species, shown in Fig. 9(b). It should be noted that for the atom species with lower atomic number (Ar/Ne), the amount of measurements point was too limited for a rigorous statistical analysis.

A subset of 18 samples was measured two months after irradiation testing. We observed $\mathrm{V_t}$ shifts, both positive and negative, and spikes in $\mathrm{I_g}$ for forward-gate bias, both shown on Fig. 11. Since there was a large time in between the irradiation testing and postirradiation testing, we can assume that the $\mathrm{V_t}$ shift was nonrecoverable. The spikes might indicate that after irradiation, a percolation path was formed through the gate insulation; indeed, the spiked current behavior is indicative of a phenomenon of electron tunneling through defects [12]. The characteristics of 12 samples out of the population of 18 that were measured po-

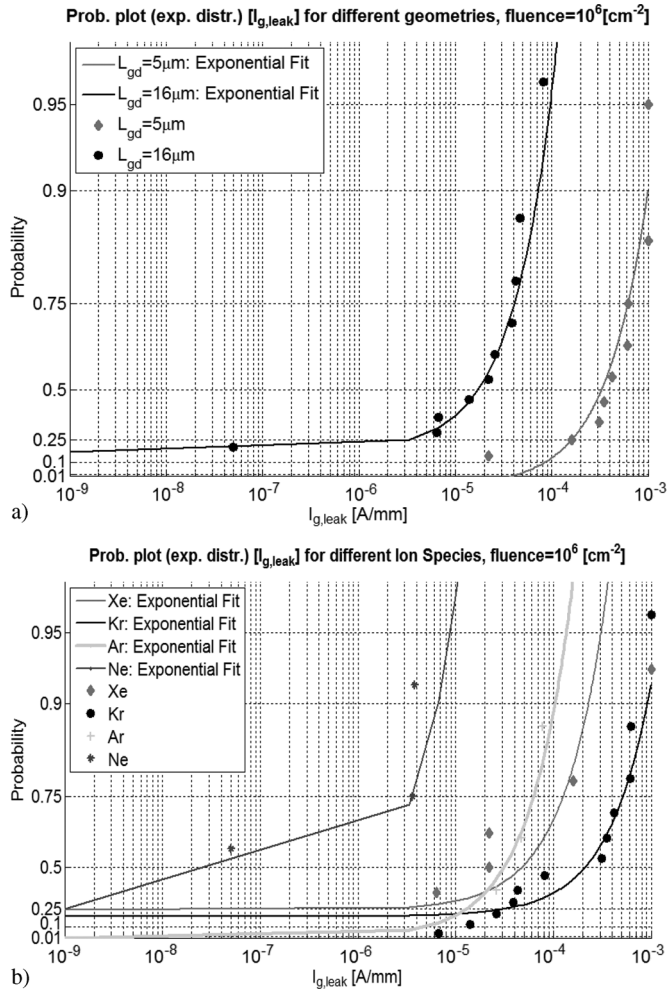

Fig. 9. Probability plot for an exponential distribution, calculated for the leakage current after irradiation ($I_{g,leak}$). Typical values before irradiation were 10^{-10} A/mm. Probability plot a) for different gate–drain geometries at a fluence of 10^6 [cm^{-2}], b) for different ion species at a fluence of 10^6 [cm^{-2}].

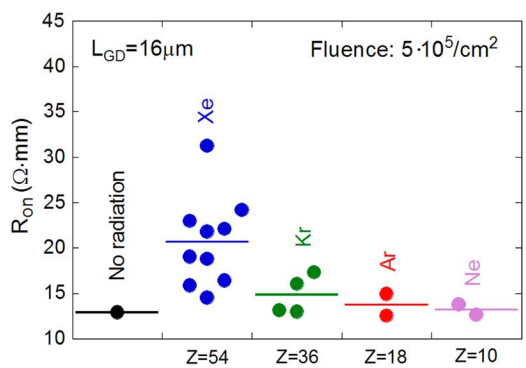

Fig. 10. Degradation of the on-resistance for irradiation with different atom species.

stirradiation exhibited the spiked behavior. However, both the V_{th} shift and the noisy forward gate current did not show any correlation in magnitude with any of the parameters, which were varied (i.e., atom species/V_{ds}/V_{gs}).

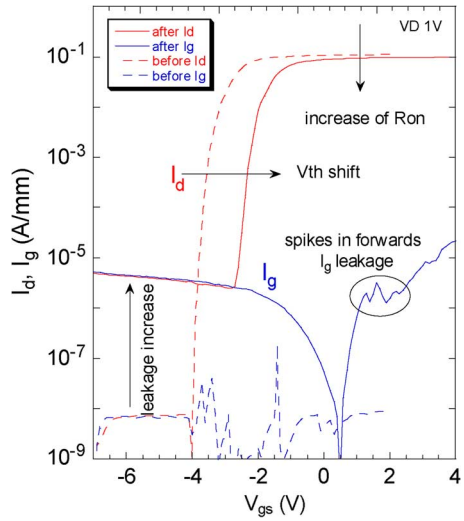

Fig. 11. Transfer-characteristic measured before (blue) and after (red) the radiation experiment with Xe and applied $VDS = 384$ V, $VGS = -8$ V. In the figure, the degradation effects induced by radiation are highlighted.

IV. Discussion

The occurrence of SES events has not been observed in previous work on AlGaN/GaN HEMT structures [3]–[6], [8]; on the contrary, authors always report that the AlGaN/GaN structures are extremely hard for SEB events.

This is the first time, to the best of our knowledge, that a GaN MISHEMT architecture has been subjected to radiation testing. Previous work on GaN HEMT radiation hardness was always performed on Schottky gate architectures [3]–[6], [8]. For the depletion-mode MISHEMTs, studied in this work, we could observe both SEGR and SES events. Due to the SEGR events, a progressive gate degradation could be observed with increasing dose and electric fields present in the component (as observed by increasing V_{ds} or varying L_{gd}). The increase in gate degradation due to SEGR is in agreement with what was found in previous work [3]–[6], [8].

The capture cross section for the SES events was not constant, as would be expected for silicon MOSFETs [9], but was linked to the gate leakage. Above a certain threshold gate leakage level, no further SES events were observed.

We propose the hypothesis that the accumulated charge at the gate is responsible for the switching events. We base the hypothesis on the fact that SES events occur that partially turn on the transistor during irradiation, and this partial switching is possible by modifying the gate potential. Furthermore, the capture cross section for the SES events is close in the value to the area of the gate in the components. The voltage dependence of the SES capture cross section could indicate that the depletion region (which extends with voltage) could also play a role.

To understand these effects, we have considered possible trails for the heavy ions to follow through the structure, shown schematically in Fig. 12. The ions can traverse through the active regime in one of the access regions (source or drain) or pass through the gate regime. It is well known that a heavy ion passing through a crystal lattice leaves an electron–hole plasma in its wake [9]. These generated carriers can have several effects. First, under the influence of the electric fields present

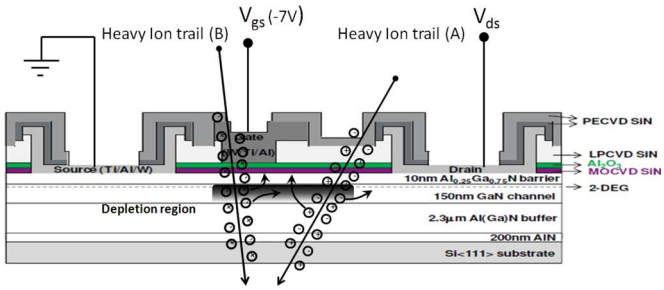

Fig. 12. Cross section of a AlGaN/GaN MISHEMT component and possible trails for heavy ions through the depletion region or the gate area.

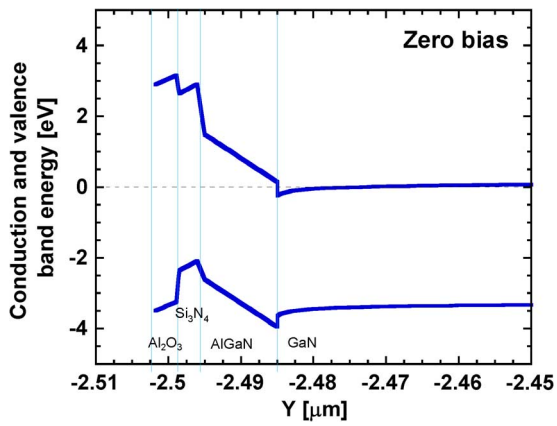

Fig. 13. Banddiagram of the MISHEMT structure, the cross section is taken through the gate area.

in the component, the generated carriers can be transported to different electrodes and either flow out through these electrodes or recombine in an area of the component with a high amount of charge carriers. For the case of the GaN MISHEMT, Fig. 12, electrons are attracted to the drain electrode, which is at high potential, and holes get attracted to the gate electrode, which is at the lowest potential. However, the transport of the charge carriers alone cannot explain the long events observed in Fig. 6(b), as the impact of the heavy ion happens on a much shorter time scale, and the deposited charge is much lower. Therefore, the events are most probably related to a partial opening of the gate. This would be possible if holes are accumulated near the gate electrode or if they would neutralize surface traps at the AlGaN/ Si_3N_4 interface, shifting the Fermi-level upward. We have performed a simulation of the band diagram near the gate electrode (Fig. 13). It can be seen on this graph that there is a barrier in the valence band at the interface between AlGaN/GaN for the holes to overcome. If holes have enough energy to overcome this barrier, they can accumulate at the interface between Si_3N_4 and AlGaN or Al_2O_3. When the transistor switches on, the electron flow is confined to the 2DEG, which is present at the GaN/AlGaN interface; therefore, any holes accumulated higher in the barrier will not recombine. This could be a possible explanation for the switching events. This band diagram is different from Si components, where the dielectric is in direct contact with the channel; therefore, carriers accumulated at this interface will recombine as soon as the transistor starts to conduct current, while for the case of GaN, the holes can only recombine with electrons leaking through the gate.

A second effect could be the trapping of charge carriers in trapping sites in the active material or in the dielectrics present in the component. Microdose effects have been considered, which pose important problems in planar and trench Si power MOSFETs [13]–[15]. This microdose effect is the local deposition of charge in a dielectric when, e.g., a heavy-ion passes through [13]. When charge is deposited in the gate dielectric of a Si powerMOS, it leads to a local threshold voltage shift (formation of a parasitic transistor). The microdose effect in Si powerMOS can thus increase the leakage current by orders of magnitude [13]–[15]. Typical for the transistors exhibiting microdose effects is a hump or smeared out $I_{ds}V_{gs}$ characteristic in the subthreshold regime. However, we did not observed a double hump in the subthreshold regime, but rather a parallel shift of the Id characteristic (Fig. 11); it is thus not probable that the GaN HEMT transistor is suffering from microdose effects.

It is currently not well understood why the transistor has a threshold in the gate leakage above which no switching events occur during radiation. We suspect that it is related to an increased recombination of holes with the electrons leaking through the gate electrode. However, it is not known exactly where they recombine. Also, the transient behavior in Fig. 6(b), which can exhibit a slow or fast rise time when switching to the on- or off-state, is currently not well understood. Future experiments are needed to pinpoint the exact reason for the transient behavior.

V. Conclusion

In conclusion, we have observed that MISHEMTS exhibit nondestructive SES events when leakage currents are very low and when measured with a protection resistor. Potentially, the devices could exhibit destructive SEB when measured without protective resistor. However, the mechanism is different as for silicon POWERMOS where SEB is caused by the turn-on of a parasitic npn transistor, while for the case of GaN, it is most probably related to a gate turn-on. A threshold value for the leakage $(I_{g,tr})$ was identified above which no SES events could be observed. Above this threshold, the MISHEMTs were equally hard to SES events as Schottky HEMTs or e-mode HEMTs. A statistical analysis of the SES events indicated that the capture cross section for single events had a lognormal distribution, with a median value close to gate area and a slight voltage dependence. We hypothesize that the occurrence of the SES events could be caused by the accumulation of holes in the gate stack. Another main degradation mechanism was SEGR; however, for our case, the degradation was related in the first place to the gate dielectric and not the AlGaN barrier layer as observed in other works. We have used statistical analysis techniques, allowing us to identify several key parameters that impacted the stability of the devices under irradiation. It was found that the gate leakage degradation followed an exponential distribution law. We observed a progressive degradation of the gate dielectric for higher ion fluences, increased drain voltage, and device geometry. These results show that the electrical fields act as an acceleration factor for the radiation induced degradation and thus indicate that an important part

of the degradation is caused by the electron–hole plasma generated in the wake of the ion traversing the crystal lattice. The components were still fully functional after irradiation, albeit with a leaky gate, which was, however, still on the same order of Schottky gate HEMT components (10–100 μA/mm). Also an increase was observed in the on-resistance, which increased for the heavier ion species, probably related to either lattice damage or charge trapping in the Si_3Ni_4 passivation layer. Our test results give a first indication that the MISHEMT technology could be robust for space applications.

ACKNOWLEDGMENT

The authors acknowledge the support of S. You and S.-H. Arturo for the TCAD simulation of the GaN MISHEMT structure and X. Kang for measurements of the transistor characteristics.

REFERENCES

[1] A. Ionascut-Nedelcescu, C. Carlone, A. Houdayer, H. J. von Bardeleben, J.-L. Cantin, and S. Raymond, "Radiation hardness of gallium nitride," *IEEE Trans. Nucl. Sci.*, vol. 49, no. 6, pp. 2733–2738, Dec. 2002.

[2] X. Hu, A. P. Karmarkar, B. Jun, D. M. Fleetwood, R. D. Schrimpf, R. D. Geil, R. A. Weller, B .D. White, M. Bataiev, L. J. Brillson, and U. K. Mishra, "Proton-irradiation effects on AlGaN/AlN/GaN high electron mobility transistors," *IEEE Trans. Nucl. Sci.*, vol. 50, no. 6, pp. 1791–1796, Dec. 2003.

[3] S. Bazzoli, S. Girard, V. Ferlet-Cavrois, J. Baggio, P. Paillet, and O. Duhamel, "SEE sensitivity of a COTS GaN transistor and silicon MOSFET," in *Proc. RADECES 2007*, Sep. 10–14, 2007, pp. 1–5.

[4] R. D. Harris, L. Z. Scheick, J. P. Hoffman, T. Thrivikraman, M. Jenabi, Y. Gim, and T. Miyahari, "Radiation characterization of commercial Gan devices," in *Proc. Radiat. Effects Data Workshop (REDW)*, Jul. 25–29, 2011, pp. 1–5.

[5] A. Lidow, J. B. Witcher, and K. Smalley, "Enhancement mode gallium nitride (eGaNTM) FET characteristics under long term stress," in *Proc. GOMACTech*, 2011.

[6] A. Lidow and K. Smalley, "Radiation tolerant enhancement mode gallium nitride (eGaNTM) FET characteristics," in *Proc. GOMACTech*, 2012, pp. 1–3.

[7] M. Van Hove, S. Boulay, S. R. Bahl, S. Stoffels, X. Kang, D. Wellekens, K. Geens, A. Delabie, and S. Decoutere, "CMOS process-compatible high-power low-leakage AlGaN/GaN MISHEMT on silicon," *IEEE Electron Device Lett.*, vol. 33, no. 5, pp. 667–669, May 2012.

[8] S. Kuboyama, A. Maru, H. Shindou, N. Ikeda, T. Hirao, H. Abe, and T. Tamaru, "Single-event damages caused by heavy ions observed in AlGaN/GaN HEMTs," *IEEE Trans. Nucl. Sci.*, vol. 58, no. 6, pp. 2734–2738, Dec. 2011.

[9] A. Holmes-Siedle and L. Adams, *Handbook of Radiation Effects*, 2nd ed. London, U.K.: Oxford Univ. Press, 2002, 978-0-19-850733-8.

[10] J. Derluyn, S. Boeykens, K. Cheng, R. Vandersmissen, J. Das, W. Ruythooren, S. Degroote, M. Leys, M. Germain, and G. Borghs, "Improvement of AlGaN.GaN high electron mobility transistor structures by *in situ* deposition of a Si_3N_4 surface layer," *J. Appl. Phys.*, vol. 98, pp. 054501.1–054501.5, 2005.

[11] S. M. Ross, *Introduction to Probability and Statistics for Engineers and Scientists*, 4th ed. Burlington, MA, USA: Associated Press, 2009, 978-0-12-370483-2.

[12] R. Degraeve, B. Kaczer, and G. Groeseneken, "Degradation and breakdown in thin oxide layers: Mechanism, models and reliability prediction," *Microelectron. Rel.*, vol. 39, no. 10, pp. 1445–1460, .

[13] J. A. Felix, M. R. Shaneyfelt, J. R. Schwank, S. M. Dalton, P. E. Dodd, and J. B. Witcher, "Enhanced degradation in power MOSFET devices due to heavy ion irradiation," *IEEE Trans. Nucl. Sci.*, vol. 54, no. 6, pp. 2181–2189, Dec. 2007.

[14] M. R. Shaneyfelt, J. A. Felix, P. E. Dodd, J. R. Schwank, S. M. Dalton, J. Baggio, V. Ferlet-Cavrois, P. Paillet, and E. W. Blackmore, "Enhanced proton and neutron induced degradation and its impact on hardness assurance testing," *IEEE Trans. Nucl. Sci.*, vol. 55, no. 6, pp. 3096–3105, Dec. 2008.

[15] S. Kuboyama, A. Maru, N. Ikeda, T. Hirao, and T. Tamura, "Characterization of microdose damage caused by single heavy ion observed in trench type power MOSFETs," *IEEE Trans. Nucl. Sci.*, vol. 57, no. 6, pp. 3257–3261, Dec. 2010.